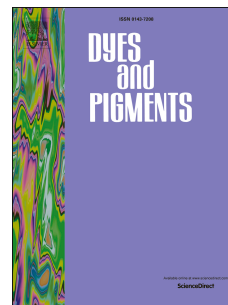


Accepted Manuscript

Near-Infrared Emitting Pyrazole-Bridged Binuclear Platinum Complexes: Synthesis, Photophysical and Electroluminescent Properties in PLEDs

Ning Su, Fanyuan Meng, Jianhua Chen, Yafei Wang, Hua Tan, Shijian Su, Weiguo Zhu



PII: S0143-7208(16)00025-5

DOI: [10.1016/j.dyepig.2016.01.014](https://doi.org/10.1016/j.dyepig.2016.01.014)

Reference: DYPI 5067

To appear in: *Dyes and Pigments*

Received Date: 20 November 2015

Revised Date: 9 January 2016

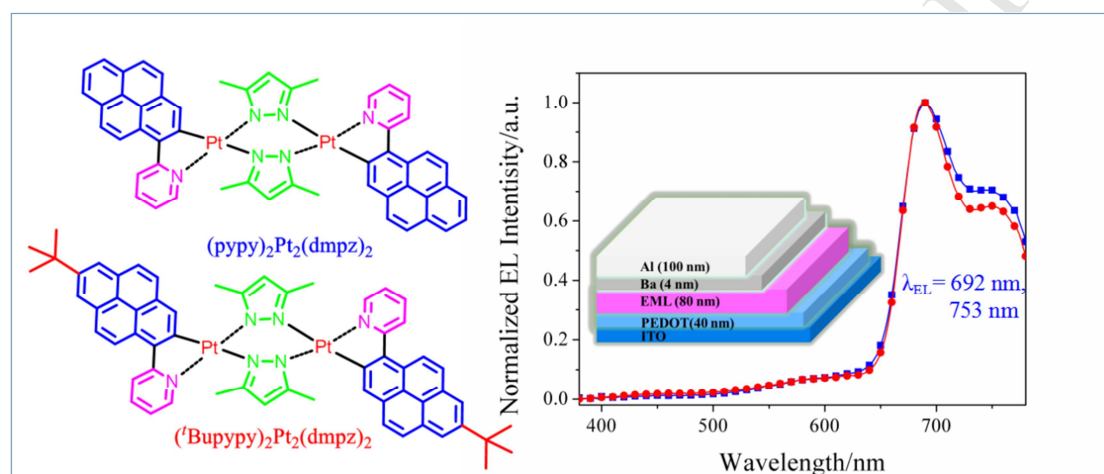
Accepted Date: 13 January 2016

Please cite this article as: Su N, Meng F, Chen J, Wang Y, Tan H, Su S, Zhu W, Near-Infrared Emitting Pyrazole-Bridged Binuclear Platinum Complexes: Synthesis, Photophysical and Electroluminescent Properties in PLEDs, *Dyes and Pigments* (2016), doi: 10.1016/j.dyepig.2016.01.014.

This is a PDF file of an unedited manuscript that has been accepted for publication. As a service to our customers we are providing this early version of the manuscript. The manuscript will undergo copyediting, typesetting, and review of the resulting proof before it is published in its final form. Please note that during the production process errors may be discovered which could affect the content, and all legal disclaimers that apply to the journal pertain.

Table of Contents

Two novel near-infrared emitting binuclear platinum (II) complexes of $(\text{ppy})_2\text{Pt}_2(\text{dmpz})_2$ and $({}^i\text{Bupppy})_2\text{Pt}_2(\text{dmpz})_2$ were synthesized. The intrinsic dual electroluminescent peaks at 692 nm and 753 nm were observed in their single-emissive-layer doped PLEDs.



**Near-Infrared Emitting Pyrazole-Bridged Binuclear Platinum
Complexes: Synthesis, Photophysical and Electroluminescent
Properties in PLEDs**

Ning Su[†], Fanyuan Meng^{†,‡}, Jianhua Chen[†], Yafei Wang^{†*}, Hua Tan[†],

Shijian Su^{†,*}, Weiguo Zhu^{†,*}

[†]College of Chemistry, Key Lab of Environment-Friendly Chemistry and Application in the Ministry of Education, Xiangtan University, Xiangtan 411105, People's Republic of China

[‡]Institute of Polymer Optoelectronic Materials and Devices, State Key Laboratory of Luminescent Materials and Devices, South China University of Technology, Guangzhou 510640, People's Republic of China

*To whom correspondence should be addressed:

(W. Z.) zhuwg18@126.com

(S. S.) mssjsu@scut.edu.cn

(Y. W.) wangyf_miracle@hotmail.com

Abstract: Two novel near-infrared emitting binuclear platinum (II) complexes were successfully designed and synthesized with the bridged ancillary ligand of 3,5-dimethyl pyrazol, in which 2-(pyren-1-yl) pyridine and its derivative of 2-(7-(*tert*-butyl)pyren-1-yl)pyridine were used as cyclometalated ligands, respectively. Their photophysical, thermal, electrochemical, as well as electroluminescent properties were investigated. The intrinsic near-infrared electroluminescent spectra peaked at 692 nm with a shoulder at 753 nm were observed in the single-emissive-layer polymer light-emitting diodes using both binuclear platinum (II) complexes as the dopant. The *tert*-butyl group attached in pyrenyl ring was found to play an important role in improving electroluminescent properties. Better electroluminescent properties were obtained for the platinum complex with 2-(7-(*tert*-butyl)pyren-1-yl)pyridine in the devices with a maximum external quantum efficiency of 0.15% and a radiant intensity of 19.10 $\mu\text{W}\cdot\text{cm}^{-2}$. To our best knowledge, this is a first reported example on the near-infrared electroluminescence of binuclear platinum complex containing pyrazoline auxiliary ligand.

Key Words: Binuclear platinum (II) complex; Near-infrared emission; Electroluminescence; Polymer light-emitting diodes

1. Introduction

Over the last two decades, platinum (II) complexes have achieved huge success in polymer/organic light-emitting diodes (PLEDs/OLEDs) due to their 100 % internal quantum efficiency and various excited states [1-7]. The strong metal-to-ligand charge transfer (MLCT) and metal-metal-to-ligand charge transfer (MMLCT) effect, as well as intermolecular interaction make these platinum (II) complexes achieve significantly red-shifted long wavelength emission, which is of considerable interest for using as near-infrared (NIR) emitting organic materials, potentially applied in bio-imaging [8-10], telecommunication [11-13], and the dissolved oxygen sensor for microbioreactors [14], especially in displays [15,16].

To date, several strategies to develop NIR emitting platinum complexes, such as expanding π -conjugation system and featuring with donor-acceptor (D-A) framework, have been demonstrated. For instance, Reynolds and his coworkers reported a series of π -extended mononuclear platinum (II) porphyrins with photoluminescent (PL) peaks ranging from 773 to 1022 nm [17]. The highest external quantum efficiency (*EQE*) of 9.2% with the maximum emission peak at 773 nm was observed in the vapor-deposited multilayer OLEDs [18]. However, the preparation of the expanded π -conjugation compounds is very complicated. Furthermore, the devices based on these planar platinum (II) porphyrins showed a serious efficiency roll-off. Considering that the intense intramolecular charge transfer (ICT) can provide remarkably red-shifted

emission in the D-A type fluorophors, we developed one D-A-A mononuclear platinum (II) complex bearing triphenylamine, benzothiadiazole and pyridine units, which displayed a NIR emission at 769 nm [19]. Although this mononuclear platinum (II) complex achieved NIR emissions through enhanced ICT effect, the device performance still has some space to be improved for their practical application.

Recently, utilization of intense MMLCT transition from platinum complexes was proved to be an effective strategy to realize NIR emission materials [20-23]. To this end, we reported a binuclear platinum (II) complex of $(\text{piq})_2\text{-Pt}_2(\mu\text{-C}_8\text{OXT})_2$ consisting of 1-phenyl-isoquinoline (piq) cyclometalated ligand and 5-(4-octyloxyphenyl)-1,3,4-oxadiazole-2-thiolate (C_8OXT) auxiliary ligand [24]. This binuclear platinum complex presented an EL emission at 702 nm with an *EQE* of 6.3% in the single-emissive-layer (SEL) PLEDs. However, it is unclear how to effectively construct Pt-Pt band and precisely control the Pt-Pt distance to achieve the MMLCT transition in these binuclear cyclometalated platinum (II) complexes.

Inspired by the intriguing photo-induced structural change leading to MMLCT transition in the pyrazolate-bridged binuclear cyclometalated platinum (II) complexes [25-26], it is expected this class of binuclear platinum (II) complexes could achieve NIR emission by enlarging cyclometalated ligand structure. In order to realize this assumption and further make clear the structure-property relationship of these pyrazolate-bridged binuclear platinum (II) complexes,

herein, we devoted our efforts to design novel NIR emission materials based on binuclear cyclometalated platinum (II) complexes containing 3,5-dimethyl-1H-pyrazol (dmpz). In this contribution, two novel pyrazolate bridged binuclear cyclometalated platinum (II) complexes of (pypy)₂Pt₂(dmpz)₂ and (^tBupypy)₂-Pt₂(dmpz)₂ were synthesized, in which 2-(pyren-1-yl) pyridine (pypy) and its *tert*-butyl derivative (^tBupypy) were used as cyclometalated ligands, respectively. Their optical, electrochemical and EL properties were primarily investigated. Isolated dual emissions at about 500 nm and 690 nm were observed for two binuclear platinum complexes in both dichloromethane solution and solid state. Employing these binuclear platinum complexes as the dopant, the single-emissive-layer PLEDs show the stable NIR emission with a peak at 692 nm and a shoulder at 753 nm at various doping concentrations from 2 wt%, 4 wt% to 8 wt%. The (^tBupypy)₂Pt₂(dmpz)₂-based PLEDs possess a better device performance with the maximum *EQE* of 0.15% and a radiant intensity of 19.10 μWcm⁻². To our best knowledge, this is the first report on the NIR PLEDs based on the pyrazolate-bridged binuclear platinum (II) complexes.

Experiments

2.1 Methods

All solvents were carefully dried and distilled prior to use. Commercially available reagents were used without further purification unless otherwise stated. All reactions were performed under nitrogen atmosphere and were monitored by thin-layer chromatography. ¹H NMR spectra were recorded on a

Bruker Avance-400 spectrometer at 400 MHz using CDCl_3 as solvent and tetramethylsilane (TMS) as the internal standard unless specified otherwise. Mass spectra were measured on a Bruker Daltonics BIFL-EX III MALDI-TOF analyzer under MALDI mode. The UV/vis absorption and PL spectra were measured with a Varian Cray 50 and Perkin-Elmer LS50B luminescence spectrometer, respectively. The equation of $\Phi_s = \Phi_r(\eta_s^2 A_r I_s / \eta_r^2 A_s I_r)$ was used to calculate the fluorescence quantum yield (Φ) of the binuclear platinum complex using complex $\text{Ru}(\text{bpy})_3$ as the standard compound in N_2 atmosphere, where Φ_s is the quantum yield of the sample, Φ_r is the quantum yield of the reference, η is the refractive index of the solvent, A_s and A_r are the absorbance of the sample and the reference at the wavelength of excitation, and I_s and I_r are the integrated areas of emission bands [27]. Fluorescence decay curves were obtained on FLS920 with time-corrected single-photon-counting (TCSPC) measurement. The thermogravimetric analysis (TGA) was performed with a NETZSCH STA449 apparatus from 25 to 600 °C at a heating rate of 10 °C/min under nitrogen atmosphere. Cyclic voltammetry measurement was conducted on a CHI620 voltammetric analyzer under argon atmosphere in an anhydrous acetonitrile solution of tetra(n-butyl) ammonium hexafluorophosphate ($\text{BuN}_4\text{-PF}_6$, 0.1 M) at a scan rate of 20 mV/s. The platinum plate, platinum wire and Ag/AgCl electrode were used as working electrode, counter electrode, reference electrode, respectively. Binuclear platinum complexes were coated on the surface of platinum plate and all potentials were corrected against ferrocene/

ferrocenium (Fc/Fc⁺).

2.2 Device fabrication and characterization

(ppy)₂Pt₂(dmpz)₂ and (Bupppy)₂Pt₂(dmpz)₂ were dissolved in chlorobenzene with a concentration of 5mg/mL at room temperature overnight. Firstly, poly(ethylenedioxythiophene)/poly(styrenesulfonate) (PEDOT:PSS) was spin-coated on indium tin oxide (ITO) at 3000 rpm in N₂ atmosphere. Then the emissive layer consisting of polyvinylcarbazole (PVK) and 1,3-bis(5-(4-(*tert*-butyl)phenyl)-1,3,4-oxadiazol-2-yl)benzene (OXD-7) was prepared by spin-coating at 1500 rpm in N₂ atmosphere. Finally, 4 nm cathode of Ba and 100 nm capping layer of Al were successively deposited on the top of emissive layer through a shadow mask in vacuum. The device structure is ITO/ PEDOT: PSS (40 nm)/ binuclear platinum complex (x%) + PVK:OXD-7 (50 nm)/ Ba (4 nm)/ Al (100 nm). The doping concentrations of binuclear platinum complexes were 2 wt%, 4 wt% and 8 wt% in the emissive layer, respectively. The ratio of PVK and OXD-7 was 7:3 in weight. The EL spectra were recorded on miniature fiberoptic spectrometer (USB 2000, Ocean Optics). The current density-voltage-radiant emittance (*J-V-R*) characteristics were recorded on a Keithley 236 source measurement unit and a calibrated silicon photodiode. And *EQE* values were calculated based on the reported procedure [28].

2.4 Synthesis of (ppy)₂Pt₂(dmpz)₂

To a suspension of K₂PtCl₄ (446 mg, 1.08 mmol) in 2-ethoxyethanol (15mL) and water (5 mL), compound **3a** (ppy) (600 mg, 2.15 mmol) were added under

N₂ atmosphere. The mixture was stirred at 80 °C for 24 h. After cooled to room temperature (RT), the mixture was poured into water (50 mL) and the precipitate was collected and washed with water (2 × 10 mL). The crude precipitate was dried in vacuum for 2 h to give chloro-bridged dimer as dark yellow solid (750 mg). This dimer was directly used to next step without any further purification.

A mixture of chloro-bridged dimer (750 mg, 0.67 mmol), 3,5-dimethylpyrazole (dmpz) (128 mg, 1.33 mmol) and CH₃ONa (362 mg, 6.7 mmol) in dichloromethane (DCM) was stirred at 60 °C for 48 h under N₂ atmosphere. After cooled to RT, the suspension was distilled to remove solvent under reduced pressure. The crude was purified through a flash silica gel column using petroleum ether (PE)/DCM (V/V = 2/1) as the eluent to give (pypy)₂Pt₂(dmpz)₂ as light yellow solid in a yield of 34%. ¹H NMR (400 MHz, CDCl₃) δ ppm: 8.71 (d, *J* = 1.5 Hz, 2H), 8.60 (d, *J* = 7.6 Hz, 2H), 8.25 (d, *J* = 6.3 Hz, 2H), 8.09-7.99 (m, 6H), 7.96-7.89 (m, 6H), 7.84 (s, 2H), 7.74 (s, 2H), 6.97 (s, 2H), 6.13 (s, 2H), 2.47 (s, 6H), 2.24 (d, *J* = 14.6 Hz, 6H). MALDI-MS (*m/z*) for C₅₂H₃₈N₆Pt₂: calcd. 1137.25; found, 1136.317.

2.5 Synthesis of (‘Bupypy)₂Pt₂(dmpz)₂

(‘Bupypy)₂Pt₂(dmpz)₂ was synthesized according to the above synthetic procedure of (pypy)₂Pt₂(dmpz)₂ as dark yellow solid with a yield of 30%. ¹H NMR (400 MHz, CDCl₃) δ ppm: 8.70 (d, *J* = 3.7 Hz, 2H), 8.61 (d, *J* = 9.1 Hz, 2H), 8.28 (d, *J* = 7.7 Hz, 2H), 8.11 (s, 4H), 8.02 (d, *J* = 9.2 Hz, 2H), 7.93 (d, *J*

= 8.8 Hz, 2H), 7.87 (d, $J = 8.8$ Hz, 2H), 7.80 (s, 2H), 7.78-7.71 (m, 2H), 6.97 (s, 2H), 6.12 (s, 2H), 2.46 (s, 6H), 2.25 (s, 6H), 1.55 (s, 18H). MALDI-MS (m/z) for $C_{60}H_{54}N_6Pt_2$: calcd. 1248.37; found, 1248.458.

3. Results and discussion.

3.1. Synthesis and characterization

The synthetic route of both binuclear platinum complexes is depicted in Scheme 1. Compound **2** was prepared based on the reported procedure [29]. Suzuki coupling reaction between compound **2** and 2-bromopyridine afforded the cyclometalated ligand **3** (pypy or ^tBupypy) in the presence of $Pd(PPh_3)_4$ in 78% yield. The pyrazolate-bridged binuclear platinum complexes of $(pypy)_2Pt_2-(dmpz)_2$ and $(^tBupypy)_2Pt_2(dmpz)_2$ were prepared by a successive two-step reactions according to the previous reports [23, 30]. The target binuclear platinum (II) complexes were confirmed with 1H NMR and MALDI-TOF mass spectrometry (see ESI).

3.2 Photophysical properties

The UV/vis absorption spectra of $(pypy)_2Pt_2(dmpz)_2$ and $(^tBupypy)_2Pt_2-(dmpz)_2$ in DCM solution (10^{-5} M) at room temperature are shown in Fig. 1. Similar absorption spectra with two resolved absorption bands are displayed in the range of 250-500 nm. The high-energy absorption bands at about 286 nm with an extinction coefficient (ϵ) of $4.2 \times 10^5 M^{-1}cm^{-1}$ is definitely ascribed to the spin-allowed ligand-central (1LC) $\pi-\pi^*$ transition [31]. On the basis of assignments in analogous molecules [25-26], the low-energy absorption bands at

about 413 nm ($2.0 \times 10^5 \text{ M}^{-1} \text{ cm}^{-1}$) can be attributed to the spin-allowed intra-ligand (^1IL) transition and $^1\text{MLCT}$ transition, to some extent $^1\text{MMLCT}$ transition, which were found in those absorption profiles for the mononuclear platinum (II) complex containing 2-(pyren-1-yl)pyridine ligand [31] and the butterfly-like binuclear platinum (II) complexes bearing pyrazolate ligands [32]. Compared to the pyrazolate-bridged binuclear platinum complex bearing difluorophenyl pyridine, both binuclear platinum complexes here show significantly red-shifted absorption [33]. In addition, $(\text{pypy})_2\text{Pt}_2(\text{dmpz})_2$ and $(^t\text{Bupypy})_2\text{Pt}_2(\text{dmpz})_2$ further exhibit the red-shifted absorption spectra in neat films instead of in DCM, implying that a stronger intermolecular interaction exist in neat film (Fig. S1, ESI).

Fig. 2a shows the PL spectra of both binuclear platinum complexes in DCM (10^{-5} M) under the excitation wavelength of 410 nm. The relevant data are summarized in Table 1. Both binuclear platinum complexes exhibit clearly dual emission at 480 nm and 690 nm in solution under N_2 atmosphere. Based on Ma's reports, we assumed that the higher energy band is attributed to a singlet ^1LC excited state, while the lower energy band is assigned to the $^3\text{MLCT}$ excited state with a little contribution of the $^3\text{MMLCT}$ excited state to some extent [32-33]. In order to further demonstrate this assumption, we measured the PL emission at the same concentration in the air. The lower energy emission is obviously quenched by oxygen, which indicates that the emission at 690 nm origins from triplet excited state. Furthermore, significantly different emission

lifetimes between 480 nm (ca. 4.40 ns and 5.78 ns) and 690 nm (ca. 3.47 μ s and 3.84 μ s) also confirmed the different excited state for the PL spectra of (pypy)₂Pt₂(dmpz)₂ and (^tBupypy)₂Pt₂(dmpz)₂. Using Ru(bpy)₃ as the standard compound, (pypy)₂Pt₂(dmpz)₂ and (^tBupypy)₂Pt₂(dmpz)₂ show a fluorescence quantum yield of 2.58% and 5.90% in degassed DCM, respectively. In order to explore the effect of different solvent on the PL emission, we measured the PL spectra for (pypy)₂Pt₂(dmpz)₂ and (^tBupypy)₂Pt₂(dmpz)₂ in different solvents, which are showed in Fig. S2 (see ESI) together with the PL profiles of the pypy and ^tBupypy ligands in DCM. Similar PL profiles with a little blue shift are observed in different solvents with the increasing polarity for both platinum complexes. Fig. 2b further shows their PL spectra in a solid-state polystyrene (PS) matrix. In contrast to the PL profiles in DCM solutions, remarkably red-shift dual emissions centered at 527 nm and 687 nm with a shoulder at 717 nm are exhibited in the PS matrix. This result suggests that expanding π -conjugation for cyclometalated ligands can result in dual emission of their dinuclear platinum complexes in solution and solid state.

3.3 Thermal property

TGA measurement was carried out to evaluate the thermal properties of binuclear platinum complexes. The recorded TGA curve is shown in Fig. S3 (see ESI). The decomposition temperatures (T_d) of 318 °C and 277 °C are observed for (pypy)₂Pt₂(dmpz)₂ and (^tBupypy)₂Pt₂(dmpz)₂ at 5% weight loss, respectively. The grafted *tert*-butyl in pyrenyl moiety has a little negative effect

on the thermal stability of its binuclear platinum complex.

3.4. Electrochemical property

The CV curve is recorded in Fig. S4. The corresponding data are collected in Table 2. The irreversible onset oxidation potentials (E_{ox}) of (ppy)₂Pt₂(dmpz)₂ and (*t*-Bupppy)₂Pt₂(dmpz)₂ are observed at 0.27 V and 0.23 V vs Fc/Fc⁺. The highest occupied molecular orbit (HOMO) energy levels (E_{HOMO}) can be calculated according to the following equation: $E_{HOMO} = -(E_{ox} + 4.8)$ eV [34]. As a calculated result, the E_{HOMO} values are -5.07 eV and -5.03 eV for (ppy)₂Pt₂(dmpz)₂ and (*t*-Bupppy)₂Pt₂(dmpz)₂, respectively. Based on their corresponding optical energy gaps (E_g^{opt}) and E_{HOMO} levels [35], the lowest unoccupied molecular orbital (LUMO) energy levels (E_{LUMO}) are estimated to be -2.63 eV for (ppy)₂Pt₂(dmpz)₂ and -2.61 eV for (*t*-Bupppy)₂Pt₂(dmpz)₂. It indicates that the grafted *tert*-butyl has a little influence on electrochemical properties in the binuclear platinum complexes.

3.5 Electroluminescent property

Fig. 4 shows the EL spectra of the binuclear platinum complexes-based devices at the dopant concentrations of 2 wt%, 4 wt% and 8 wt%, respectively. Almost identified EL spectra are observed for both devices at the same dopant concentrations. Three isolated emission peaks located at 692 nm, 753 nm and 445 nm were detected. Compared to the PL spectrum of PVK/OXD-7(7:3) as shown in Fig. S5, the higher energy emission comes from host matrix of PVK/OXD-7 and the lower energy emission is assigned to platinum complex [36].

Therefore, the EL emission here is dominated by MMLCT transition. As increasing the dopant concentrations from 2 wt%, 4 wt% to 8 wt%, the emissive intensity at about 445 nm is remarkably decreased and up to disappeared, which demonstrates that the energy transfer from host matrix to dopant is complete in the device at high dopant concentration. Additionally, it is worth noted that the *tert*-butyl substituent plays a positive effect on the energy transfer from host matrix to guest. Fig. 5 shows the *EQE* curves of the (pypy)₂-Pt₂(dmpz)₂ and (^tBupypy)₂Pt₂(dmpz)₂-based devices at different dopant concentrations. It is found that the (pypy)₂Pt₂(dmpz)₂-based devices exhibit a decreased EL efficiency with increasing dopant concentrations from 2 wt% to 8 wt%. In contrast, the (^tBupypy)₂Pt₂(dmpz)₂-based devices display an increased EL efficiency. This result also confirmed that the bulky steric hindrance of bulky group has a crucial role on the inhibition of concentration quenching in device. The highest *EQE* values of 0.11% and 0.15 % are obtained in the (pypy)₂Pt₂(dmpz)₂- and (^tBupypy)₂Pt₂(dmpz)₂-based devices, respectively. The current density-voltage-radiant intensity (*J-V-R*) characteristics of these devices are depicted in Fig. 6, and the data are listed in Table 3. The applied voltages and log functions of current densities exhibit linear relationship while the applied voltages exceed threshold voltage value [37]. Furthermore, the maximum radiant intensity of 16.65 and 19.10 μW.cm⁻² are obtained in the (pypy)₂Pt₂(dmpz)₂- and (^tBupypy)₂Pt₂(dmpz)₂-based devices, respectively.

Conclusions

In summary, two novel 3,5-dimethylpyrazole-bridged binuclear platinum complexes of $(\text{pypy})_2\text{Pt}_2(\text{dmpz})_2$ and $({}^t\text{Bupypy})_2\text{Pt}_2(\text{dmpz})_2$ were obtained and characterized. Both binuclear platinum complexes showed similar UV-vis absorption and PL spectra, as well as the analogical electrochemical properties. Expanded π -conjugation in cyclometalated ligand can control the dual emission of its platinum complexes in solution and solid state. Furthermore, almost the same NIR EL profiles peaked at 692 nm with a shoulder at 753 nm were observed in the PLEDs using both binuclear platinum complexes as the dopant, respectively. Significantly improved EL properties were obtained in the $({}^t\text{Bupypy})_2\text{Pt}_2(\text{dmpz})_2$ -doped devices with a *EQE* of 0.15% and a radiant intensity of $19.10 \mu\text{W}\cdot\text{cm}^{-2}$. This work proves an efficient strategy for binuclear platinum complexes to give the NIR EL emission by MMLCT effect in PLEDs.

Acknowledgments

Thanks to the financial supports from the National Natural Science Foundation of China (51473140, 21202139, 51273168), the Program for Innovative Research Cultivation Team in University of Ministry of Education of China (1337304), the Innovation Group in Hunan Natural Science Foundation (12JJ7002), Natural Science Foundation of Hunan (2015JJ2139, 12JJ4019), the Scientific Research Fund of Hunan Provincial Education Department (12B123, 11CY023), the Scientific Research Fund of Xiangtan University (11QDZ18, 2011XZX08).

Appendix A. Supplementary material

Supplementary data related to this article can be found at -----.

Reference

- [1] Li JY, Ma CW, Tang JX, Lee CS, Lee ST. Novel starburst molecule as a hole injecting and transporting material for organic light-emitting devices. *Chem Mater* 2005; 17: 615-619.
- [2] Fave C, Cho TY, Hissler M, Chen CW, Luh TY, Wu CC, Réau R. First examples of organophosphorus-containing materials for light-emitting diodes. *J Am Chem Soc* 2003; 125: 9254-9255.
- [3] Ding BF, Alameh K. High-contrast tandem organic light-emitting devices employing semitransparent intermediate layers of LiF/Al/C₆₀. *J Phys Chem C* 2012; 116: 24690-24694.
- [4] Nau S, Schulte N, Winkler S, Frisch Johannes, Vollmer A, Koch N, Sax S, J. W. List E. Highly efficient color-stable deep-blue multilayer PLEDs: preventing PEDOT: PSS-induced interface degradation. *Adv Mater* 2013; 25: 4420-4424.
- [5] Cummings SD, Eisenber R. Tuning the excited-state properties of platinum (II) diimine dithiolate complexes. *J Am Chem Soc* 1996; 118, 1949-1960.
- [6] Connick WB, Geiger David, Eisenberg R. Excited-state self-quenching reactions of square planar platinum (II) diimine complexes in room-temperature fluid solution. *Inorg Chem* 1999; 38: 3264-3265.
- [7] Pomestchenko IE, Castellano FN. Solvent switching between charge transfer and intra-ligand excited states in a multi-chromophoric platinum (II) complex. *J Phys Chem A* 2004; 108: 3485-3492.

- [8] Mauro M, Aliprandi A, Septiadi D, Kehr NS, Cola LD. When self-assembly meets miology: Luminescent platinum complexes for imaging applications. *Chem Soc Rev* 2014; 43: 4144-4166.
- [9] Septiadi D, Aliprandi A, Mauro M, Cola LD. Bio-imaging with neutral luminescent Pt(II) complexes showing metal/metal interactions. *RSC Adv* 2014; 4: 25709-25718.
- [10] Guo ZQ, Nam SW, Park SS, Yoon JY. A highly selective ratiometric near-infrared fluorescent cyanine sensor for cysteine with remarkable shift and its application in bioimaging. *Chem Sci* 2012; 3: 2760-2765.
- [11] Tessler N, Medvedev V, Kazes M, Kan SH, Banin U. Efficient near-infrared polymer nanocrystal light-emitting diodes. *Science* 2002; 295: 1506-1508.
- [12] Stouwdamand JW, van Vegge Frank C. J. M. Near-infrared emission of redispersible Er^{3+} , Nd^{3+} , and Ho^{3+} doped LaF_3 nanoparticles. *Nano Lett* 2002; 2: 734-737.
- [13] Tanabe S, Feng X. Temperature variation of near-infrared emission from Cr^{4+} in aluminate glass for broadband telecommunication. *Appl Phys Lett* 2000; 77: 818-820.
- [14] Jin PW, Chu J, Miao Y, Tan J, Zhang SL, Zhu WH. A NIR luminescent copolymer based on platinum porphyrin as high permeable dissolved oxygen sensor for microbio- reactors. *AIChE J* 2013; 59: 2743-2752.
- [15] Huang X, El-Sayed IH, Qian W, El-Sayed MA. Cancer cell imaging and photothermal therapy in the near-infrared region by using gold nanorods. *J Am Chem Soc* 2006; 128: 2115-2120.
- [16] Frangioni JV. In vivo near-infrared fluorescence imaging. *Curr Opin Chem Biol* 2003; 7: 626-634.

- [17] Sommer JR, Shelton AH, Parthasarathy A, Ghiviriga I, Reynolds JR, Schanze KS. Photophysical properties of near-infrared phosphorescent π -extended platinum porphyrins. *Chem Mater* 2011; 23: 5296-5304.
- [18] Graham KR, Yang YX, Sommer JR, Shelton AH, Schanze KS, Xue JG, Reynolds JR. Extended conjugation platinum (II) porphyrins for use in near-infrared emitting organic light emitting diodes. *Chem Mater* 2011; 23: 5305-5312.
- [19] Yu JT, He KQ, Li YH, Tan H, Zhu MX, Wang YF, Liu Y, Zhu WG, Wu HB. A novel near-infrared-emitting cyclometalated platinum (II) complex with donore-acceptore-acceptor chromophores. *Dyes and Pigments* 2014; 107: 146-152.
- [20] Guo ZQ, C. W. Chan M. Shape-persistent binuclear cyclometalated platinum (II) luminophores: pushing p-mediated excimeric fluid emissions into the NIR region and ion-induced perturbations. *Chem Eur J* 2009; 15: 12585-12588.
- [21] Lu W, C. W. Chan M, Zhu NY, Che CM, Li C, Hui Z. Structural and spectroscopic studies on Pt^{III}Pt and π - π interactions in luminescent multinuclear cyclometalated platinum (II) homologues tethered by oligophosphine auxiliaries. *J Am Chem Soc* 2004; 126: 7639-7651.
- [22] Sicilia V, Forniés J, Casas JM, Martín A, López JA, Larraz C, Borja P, Ovejero C, Tordera D, Bolink H. Highly luminescent half-lantern cyclometalated platinum (II) complex: synthesis, structure, luminescence studies, and reactivity. *Inorg Chem* 2012; 51: 3427-3435.
- [23] Kato M, Omura A, Toshikawa A, Kishi S, Sugimoto Y. Vapor-induced luminescence switching in crystals of the syn-isomer of a dinuclear (bipyridine) platinum (II) complex bridged with pyridine-2-thiolate ions. *Angew Chem Int Ed* 2002; 41: 3183-3185.

- [24] Wu XG, Liu Y, Wang YF, Wang L, Tan H, Zhu MX, Zhu WG, Cao Y. Highly efficient near-infrared emission from binuclear cyclometalated platinum complexes bridged with 5-(4-octyloxyphenyl)-1,3,4-oxadiazole-2-thiol in PLEDs. *Org Electron* 2012; 13: 932-937.
- [25] Ma BW, Djurovich PI, Garon S, Alleyne B, Thompson ME. Platinum binuclear complexes as phosphorescent dopants for monochromatic and white organic light-emitting diodes. *Adv Funct Mater* 2006; 16: 2438-2446.
- [26] Chakraborty A, Deaton JC, Haefele A, Castellano FN. A charge-transfer and ligand-localized photophysics in luminescent cyclometalated pyrazolate-bridged dinuclear platinum (II) complexes. *Organometallics* 2013; 32: 3819-3829.
- [27] Li Jian, Djurovich PI, Alleyne BD, Yousufuddin M, Ho NN, Thomas JC, Peters JC, Rand B, Thompson ME. Synthetic control of excited-state properties in cyclometalated Ir (III) complexes using ancillary ligands. *Inorg Chem* 2005; 44: 1713-1726.
- [28] Tamayo AB, Alleyne BD, Djurovich PI, Lamansky S, Tsyba I, Ho NN, Bau R, Thompson ME. Synthesis and characterization of facial and meridional tris-cyclometalated iridium (III) complexes. *J Am Chem Soc* 2003; 125: 7377-7387.
- [29] Figueira-Duarte TM, Simon SC, Wagner M, Druzhinin SI, Zachariasse KA, Müllen K. Polypyrene dendrimers. *Angew Chem* 2008; 120: 10329-10332.
- [30] Ghavale N, Wadawale A, Dey S, Jain VK. Synthesis, structures and spectroscopic properties of platinum complexes containing orthometalated 2-phenylpyridine. *J Organomet Chem* 2010; 695: 1237-1245.

- [31] Wu WT, Wu WH, Ji SM, Guo HM, Zhao JZ. Observation of room-temperature deep-red/near-IR phosphorescence of pyrene with cycloplatinated complexes: an experimental and theoretical study. *Eur J Inorg Chem* 2010; 4470-4482.
- [32] Zhou CK, Tian Y, Yuan Z, Han MG, Wang JM, Zhu L, Tameh MS, Huang C, Ma BW. Precise design of phosphorescent molecular butterflies with tunable photoinduced structural change and dual emission. *Angew Chem Int Ed* 2015; 54: 9591-9595.
- [33] Han MG, Tian Y, Yuan Z, Zhu L, Ma BW. A phosphorescent molecular “butterfly” that undergoes a photoinduced structural change allowing temperature sensing and white emission. *Angew Chem Int Ed* 2014; 53: 10908-10912.
- [34] He KQ, Wang XD, Yu JT, Jiang HG, Xie GS, Tan H, Liu Y, Ma DG, Wang YF, Zhu WG. Synthesis and optoelectronic properties of novel fluorene-bridged dinuclear cyclometalated iridium (III) complex with A-D-A framework in the single-emissive-layer WOLEDs. *Org Electron* 2014; 15: 2942-2949.
- [35] Yu JT, Luo J, Chen Q, He KQ, Meng FY, Deng XP, Wang YF, Tan H, Jiang HG, Zhu WG. Synthesis and optoelectronic properties of a novel dinuclear cyclometalated platinum (II) complex containing triphenylamine-substituted indolo[3,2-b]carbazole derivative in the single-emissive-layer WPLEDs. *Tetrahedron* 2014; 70: 1246-1251.
- [36] He Z, Wong WY, Yu XM, Kwok HS, Lin ZY. Phosphorescent platinum (II) complexes derived from multifunctional chromophores: Synthesis, structures, photophysics, and electroluminescence. *Inorg Chem* 2006; 45: 10922-10937.
- [37] Varker CJ, Ravi KV. Oxidation-induced stacking faults in silicon. II. electrical effects in P N diodes. *J Appl Phys* 1974; 45: 272-287.

Captions of Figures

Scheme 1. Synthetic route of $(\text{ppy})_2\text{Pt}_2(\text{dmpz})_2$ and $({}^t\text{Bupppy})_2\text{Pt}_2(\text{dmpz})_2$.

Fig. 1. UV/vis absorption spectra of $(\text{ppy})_2\text{Pt}_2(\text{dmpz})_2$ and $({}^t\text{Bupppy})_2\text{Pt}_2(\text{dmpz})_2$ in dilute DCM (10^{-5} M) at room temperature.

Fig. 2. PL spectra of $(\text{ppy})_2\text{Pt}_2(\text{dmpz})_2$ and $({}^t\text{Bupppy})_2\text{Pt}_2(\text{dmpz})_2$ in dilute DCM solution (10^{-5} M) (a) and in the polystyrene film (b) at room temperature.

Fig. 3. Fluorescence decay curves of $(\text{ppy})_2\text{Pt}_2(\text{dmpz})_2$ and $({}^t\text{Bupppy})_2\text{Pt}_2(\text{dmpz})_2$ in dilute DCM (10^{-5} M) monitored at wavelength of 480 nm and 690 nm in N_2 atmosphere.

Fig. 4. EL spectra of the $(\text{ppy})_2\text{Pt}_2(\text{dmpz})_2$ - and $({}^t\text{Bupppy})_2\text{Pt}_2(\text{dmpz})_2$ -based devices at different dopant concentrations from 2 wt% to 8 wt%.

Fig. 5. *EQE* curves of the $(\text{ppy})_2\text{Pt}_2(\text{dmpz})_2$ - and $({}^t\text{Bupppy})_2\text{Pt}_2(\text{dmpz})_2$ -based devices at different dopant concentrations from 2 wt% to 8 wt%.

Fig. 6. *J-V-R* profiles of the $(\text{ppy})_2\text{Pt}_2(\text{dmpz})_2$ - and $({}^t\text{Bupppy})_2\text{Pt}_2(\text{dmpz})_2$ -based devices at different dopant concentrations from 2 wt% to 8 wt%.

Table 1. Photophysical, excited state decay and thermal data of $(\text{ppy})_2\text{Pt}_2(\text{dmpz})_2$ and $({}^t\text{Bupppy})_2\text{Pt}_2(\text{dmpz})_2$.

Table 2. Electrochemical data of $(\text{ppy})_2\text{Pt}_2(\text{dmpz})_2$ and $({}^t\text{Bupppy})_2\text{Pt}_2(\text{dmpz})_2$.

Table 3. EL, *J-V-R* and *EQE* data of $(\text{ppy})_2\text{Pt}_2(\text{dmpz})_2$ and $({}^t\text{Bupppy})_2\text{Pt}_2(\text{dmpz})_2$.

Scheme 1

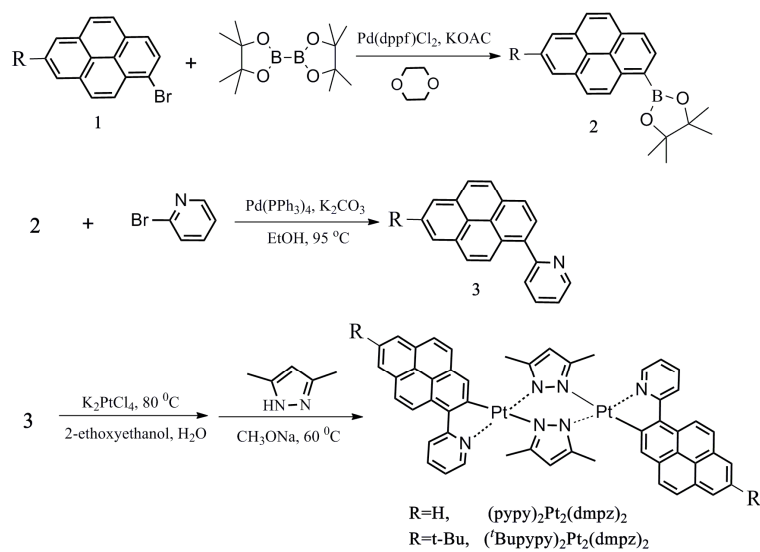


Fig. 1

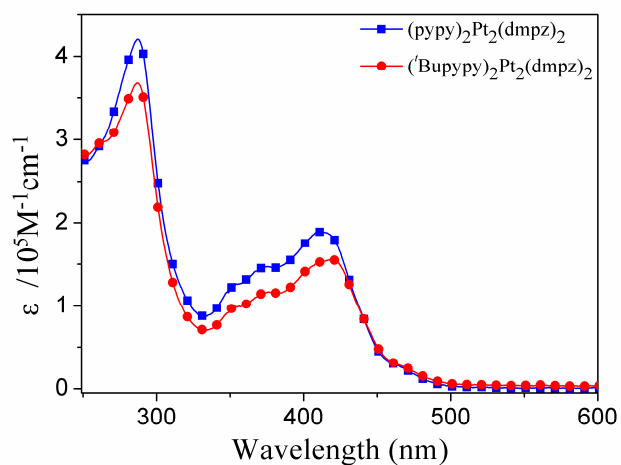
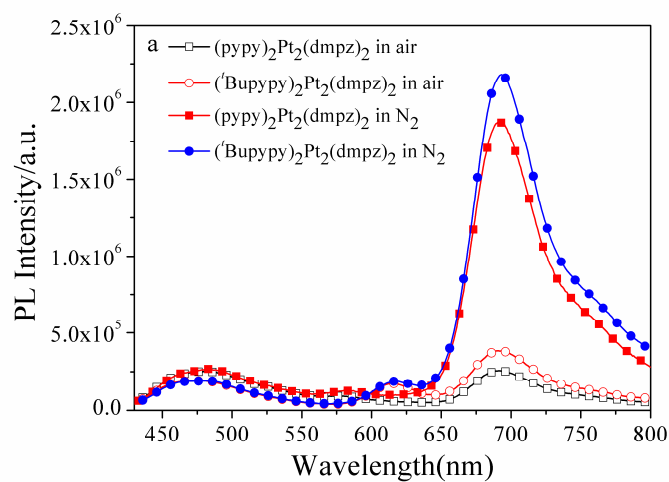


Fig. 2



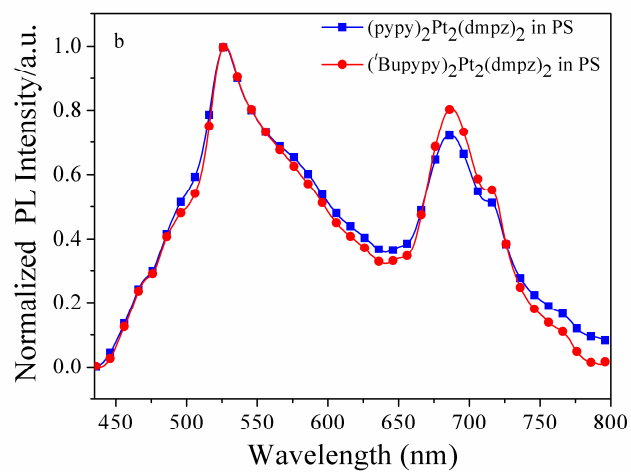


Fig. 3

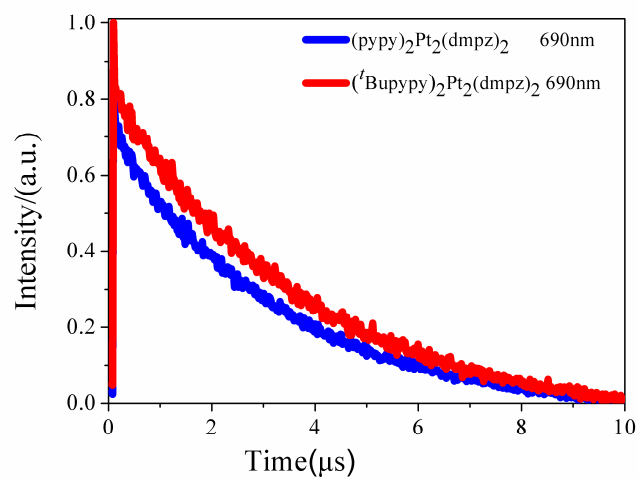
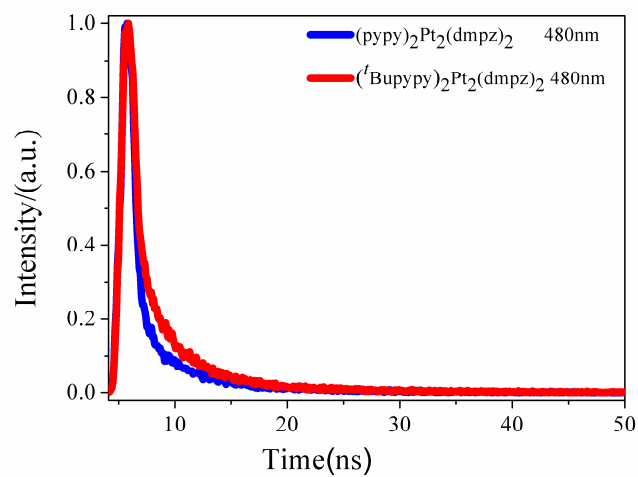


Fig. 4

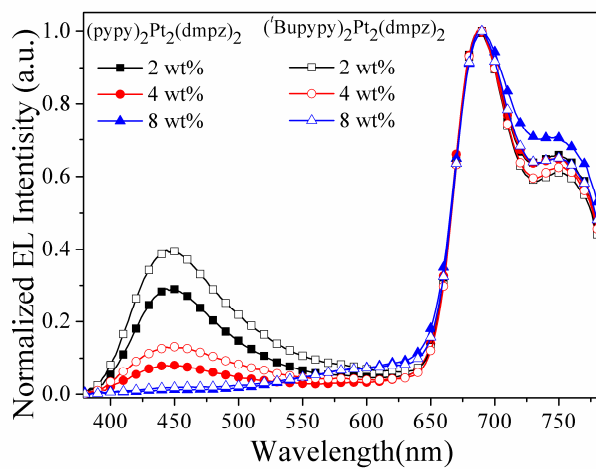
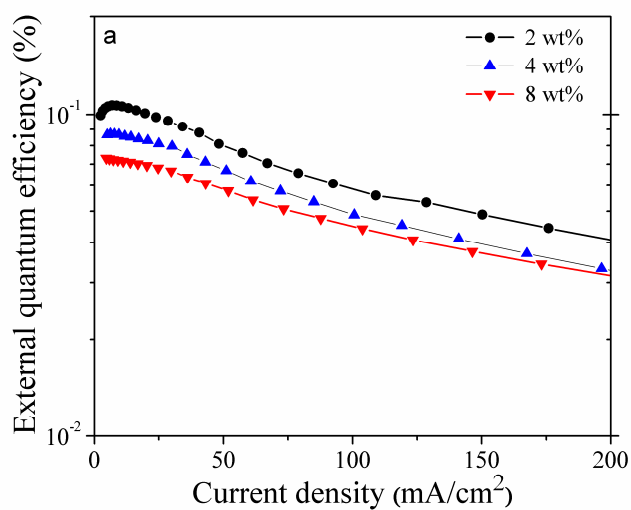


Fig. 5



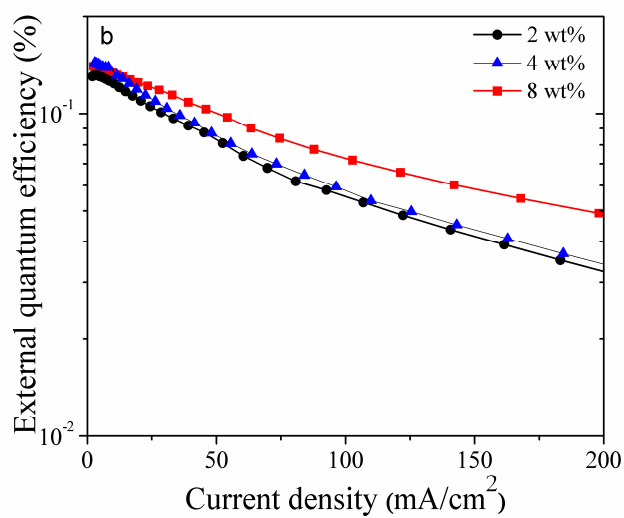


Fig. 6

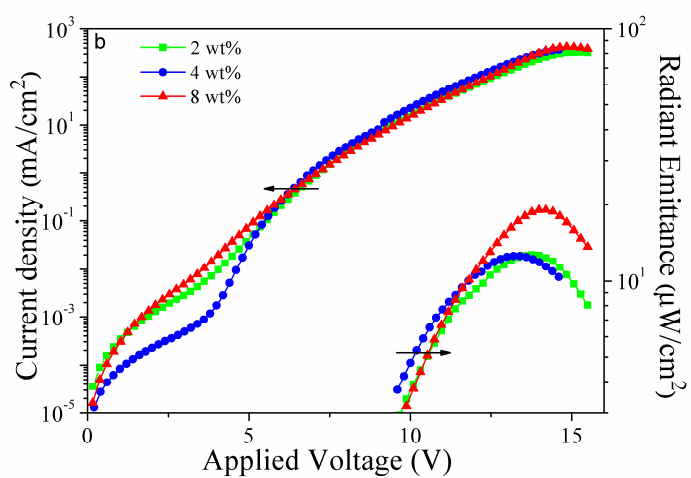
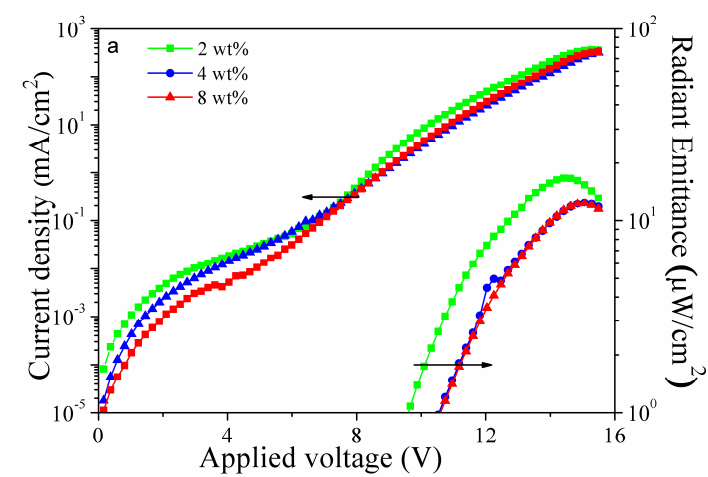


Table 1

Complexes	λ_{ab}/nm^a ($\epsilon/10^5 M^{-1} cm^{-1}$)	λ_{ab} (nm) ^b	λ_{PL} (nm) ^a	λ_{PL} (nm) ^c	Φ^d	τ^e	T_d (°C)
(ppy) ₂ Pt ₂ (dmpz) ₂	286 (4.20),	289	480	526	2.58%	4.40 ns	318
	370 (1.44),	423	577	686		3.47 μ s	
	410 (1.87)		690	715			
^t (Bupppy) ₂ Pt ₂ (dmpz) ₂	286 (3.65),	289	480	526	5.90%	5.78 ns	277
	371 (1.19),	425	614	687		3.84 μ s	
	413 (1.56)		690	717			

^a Measured in dilute DCM (10^{-5} M) at room temperature. ^b Measured in neat film at room temperature. ^c Measured in polystyrene(PS) film. ^d Measured in dilute DCM (10^{-5} M) in N₂ atmosphere according to the equation of $\Phi_s = \Phi_i(\eta_s^2 A_r I_s / \eta_r^2 A_s I_r)$. ^e Measured in dilute DCM (10^{-5} M) in N₂ atmosphere at wavelength of 480 nm and 690 nm, respectively.

Table 2

Complexes	$E_{ox}(V)^a$	$E_g^{opt}(eV)^b$	$E_{HOMO}(eV)^c$	$E_{LOMO}(eV)^d$
(ppy) ₂ Pt ₂ (dmpz) ₂	0.27	2.44	-5.07	-2.63
^t (Bupppy) ₂ Pt ₂ (dmpz) ₂	0.23	2.42	-5.03	-2.61

^a The potential of Fc/Fc⁺ vs Ag/AgCl electrode was measured to be 0.42 V. ^b Calculated from the absorption band edge of the films, $E_g^{opt} = 1240/\lambda_{edge}$. ^c Calculated from empirical equation: $E_{HOMO} = -(E_{ox} + 4.8)eV$. ^d Calculated from $E_{LUMO} = E_g^{opt} + E_{HOMO}$.

Table 3

Complexes	Ratio (%)	V_{th} (V)	R_{max} ($\mu W.cm^{-2}$)	PLQY (%) ^a	EQE_{max} (%)
(ppy) ₂ Pt ₂ (dmpz) ₂	2	9.23	16.65	0.1	0.11
	4	10.52	12.38	0.6	0.09
	8	10.31	12.24	0.4	0.07
^t (Bupppy) ₂ Pt ₂ (dmpz) ₂	2	7.93	12.74	0.1	0.13
	4	8.80	12.48	0.8	0.15
	8	8.10	19.10	0.9	0.14

^a Absolute quantum yield measured in a PVK/OXD-7(70:30) film.

Highlights

- Two pyrazolate-bridged based binuclear platinum complexes are prepared.
- Both platinum complexes show a dual emission at 480 and 690 nm in solution and thin film.
- NIR emission peak at 692 nm with a shoulder at 753 nm is observed in the platinum complexes-doped PLEDs.
- The maximum *EQE* of 0.15% and a radiant intensity of $19.10 \mu\text{Wcm}^{-2}$ are obtained in their doped PLEDs.